Laser Physics

PAPER

Laser frequency stabilization on $5P \rightarrow 5D$ transition by double resonance optical pumping and two-photon transition spectroscopy in rubidium

IOP Publishing | Astro Ltd Laser Physics
Laser Phys. **30** (2020) 025201 (6pp) https://doi.org/10.1088/1555-6611/ab5e25

Laser frequency stabilization on $5P \rightarrow 5D$ transition by double resonance optical pumping and two-photon transition spectroscopy in rubidium

Jinpeng Yuan[1,2], Shichao Dong[1,2], Lirong Wang[1,2], Liantuan Xiao[1,2] and Suotang Jia[1,2]

[1] State Key Laboratory of Quantum Optics and Quantum Optics Devices, Institute of Laser Spectroscopy, Shanxi University, Taiyuan 030006, People's Republic of China
[2] Collaborative Innovation Center of Extreme Optics, Shanxi University, Taiyuan 030006, People's Republic of China

E-mail: wlr@sxu.edu.cn

Received 25 November 2019
Accepted for publication 30 December 2019
Published 20 December 2019

Abstract

We present a laser frequency locking scheme for the high excited transition of rubidium, which cannot be directly referenced by atomic absorption spectroscopy. Double resonance optical pumping spectroscopy and two-photon transition spectroscopy of a $5S \rightarrow 5P \rightarrow 5D$ transition are obtained in a room temperature vapor cell and employed as the reference sources. An Allan deviation of 1.71×10^{-12} at an averaging time of 2048 s with a residual frequency fluctuation of ± 0.2 MHz over 7000 s is obtained by two-photon transition spectroscopy. The case of double resonance optical pumping spectroscopy presents an Allan deviation of 4.86×10^{-12} at an averaging time of 2048 s with a residual frequency fluctuation of ± 0.4 MHz over 7000 s. One distinct advantage of two-photon transition spectroscopy method is demonstrated by the analysis of the fast Fourier transform of error signal. A narrower full width at half-maximum of two-photon transition spectroscopy and a higher zero crossing slope by using a frequency modulation method lead to a better frequency stabilization. This work provides a technical basis for the laser frequency stabilization based on atomic and molecular transition spectroscopy, and it also supplies a new frequency standard for optical telecommunication applications.

Keywords: frequency stabilisation, rubidium atom, laser spectroscopy

(Some figures may appear in colour only in the online journal)

1. Introduction

The manipulation of atomic and molecular systems has directly benefited from the improvement of continuous-wave laser stability over the past several decades. Especially, frequency stable continuous-wave lasers have played, and continue to play, a major role in advancing precision measurements, such as laser spectroscopy [1], quantum optics [2] and gravitational wave detection [3]. The free running linewidth, or short-term frequency stability of a laser, is often not adequate for many applications. The laser frequency stability is generally subject to various noises, and it can be improved by locking to some stable reference sources. The conventional frequency reference source includes the atomic and molecular transitions [4–7], ultra-stable reference cavity [8] and femtosecond optical frequency comb [9]. The latter two reference sources are nearly arbitrary, which leads to freedom in the choice of reference. However, they suffer from other limitations. Locking to a reference cavity will inevitably add a noticeable frequency drift to the result, which comes from the mechanical

design and the external temperature variation of the reference sources. To eliminate the frequency drift, the cavity length is often further stabilized to a spectral line and the cavity is carefully isolated [10]. The complexity and large expense of femtosecond optical comb undoubtedly limit the wide adoption in laser frequency locking. The reference source from atomic and molecular transitions achieves the basic frequency stabilization at room temperature [11]. In addition to this, compared to the cavity and optical frequency comb, this reference is also low in cost and the device is easy to adjust. Also, establishing an atomic frequency standard facilitates the experimental result evaluation in atom-related experiments. In our previous work on constructing electromagnetically induced grating [12, 13], the atomic transition lines provided a convenient reference for rapid qualitative analysis about the experimental results. These advantages make atomic and molecular transitions routinely used in most of the challenging precision measurements [14] and optical frequency standards [15–17].

Recently, the $5S \rightarrow 5P \rightarrow 5D$ two-photon transition of rubidium was extensively studied [18] because of several merits including the strong absorption line owing to the large transition probability, the superior Doppler-free background caused by the small difference between the real energy level and the virtual energy level, and the potential application as a frequency standard in the 1.55 μm telecommunications band [19]. Research has also expanded to new areas, such as building a frequency standard [17], realization of artificial periodic structure [20], generation of the orbital angular momentum of light [21], or quantum repeater at telecommunications wavelengths [22]. In these experiments, two lasers with wavelengths of 780 nm and 776 nm are used to realize the two-photon transition. The frequency stabilization of 780 nm laser can be achieved by the rubidium atom D2 line, but the case of the 776 nm laser faces more difficulties for lacking the direct absorption line. This problem also exists in the research of Rydberg atoms [23, 24]. The establishment of the Rydberg atomic system frequency reference standard is a key step in extending the previous work on neutral atoms to the Rydberg atomic system [25].

An alternative approach, which does not suffer from the limitation but still has the advantages of the atomic line, is indirect two-photon transition spectroscopy such as double resonance optical pumping spectroscopy (DROPS) and two-photon transition spectroscopy (TPTS). Moon *et al* used DROPS to stabilize the output frequency of a 776 nm laser, and the short-term frequency stabilization is achieved by optical and electric feedback methods [26, 27]. The two-photon transition spectroscopy was investigated with variable atomic density and laser detuning, and the novel method for sum-frequency stabilization of two free running lasers was suggested [28]. An all fiber frequency standard for optical communication applications based on two-photon transition spectroscopy in rubidium at 778.1 nm was reported [29]. The frequency stabilization method of a diode laser that operates on the excited state transition of ^{87}Rb atoms was investigated and supposed to be a simple method to control the laser frequency [18]. Recently, our group realized a high signal-to-noise (SNR) TPTS at 778.1 nm with the intensity modulation method. This high SNR spectrum brings possibilities for the laser frequency locking [19].

In this paper, we present the frequency stabilization of a 776 nm laser using DROPS and TPTS in a ladder-type coherent rubidium system. The two frequency references with high SNRs are obtained and the discrimination curves are then taken by the frequency modulation method. Frequency stabilization is achieved by delivering the frequency difference signal into the laser current controller. The closed loop performance is evaluated by comparison with the residual frequency fluctuations, Allan deviations, and fast Fourier transform of the error signal. This research provides a technical basis for laser frequency stabilization with DROPS and TPTS. The potential applications cover the recent research hotspots, such as the Rydberg atom and optical fiber quantum telecommunication.

2. Experimental setup

A ladder-type coherent atomic system of ^{87}Rb is employed in this experiment. The Doppler-free configuration is achieved by two counter-propagating laser beams of 776 nm and 780 nm. The related energy levels are shown in figure 1(a). The 780 nm laser couples the $5S_{1/2} \rightarrow 5P_{3/2}$ transition and excites the atoms to the $5P_{3/2}$ state, and the 776 nm laser resonances with the $5P_{3/2} \rightarrow 5D_{5/2}$ transition. After the ^{87}Rb atoms reach the $5D_{5/2}$ level, 65% of atoms decay back to the $5P_{3/2}$ level. Then the remaining atoms have a significant probability of decaying to the $5S_{1/2}$ ground state via the intermediate $6P_{3/2}$ level by the emission of 420 nm fluorescence [30].

The experiment setup as shown in figure 1(b) consists of two single mode tunable diode lasers (DL pro, Toptica) operating at around 780 nm. One of them provides a 780 nm laser and is stabilized by saturated absorption spectroscopy on the hyperfine transition of $5S_{1/2}(F = 2) \rightarrow 5P_{3/2}(F' = 3)$. Two methods use this same locked laser of 780 nm. The 10 kHz modulation frequency, modulation amplitude and proportion-integration-differential parameters of the 780 nm laser remain unchanged during the experiment of the two methods. We monitor the residual fluctuation error signal of the 780 nm laser to ensure that the lock of the 780 nm laser keeps the same. The other one radiates the 776 nm laser and the output beam divides a weak beam from the main beam by a half-wave plate and a polarization beam splitter. The weak beam is coupled into the wavelength meter (WS-7, HighFinesse) to monitor the laser frequency. In this way, we can quickly find the approximative 776 nm laser frequency corresponding to the transition at the beginning of the experiment. The main beam overlaps with the 780 nm beam in the center of the natural rubidium vapor cell (^{85}Rb, 78%, and ^{87}Rb, 22%), which has the length of 150 mm and the diameter of 25 mm. The vapor cell is wrapped in μ-metal foil to shield the earth's magnetic field. The temperature of the vapor cell is kept at 295 K, which corresponds to a density of 5.02×10^9 cm^{-3}. The DROPS is obtained by monitoring the amplitude of the 780 nm beam after being passed through the vapor cell by a photodiode (PDA36A, Thorlabs). The resulting fluorescence is converged with two lenses, and then collected by the photomultiplier

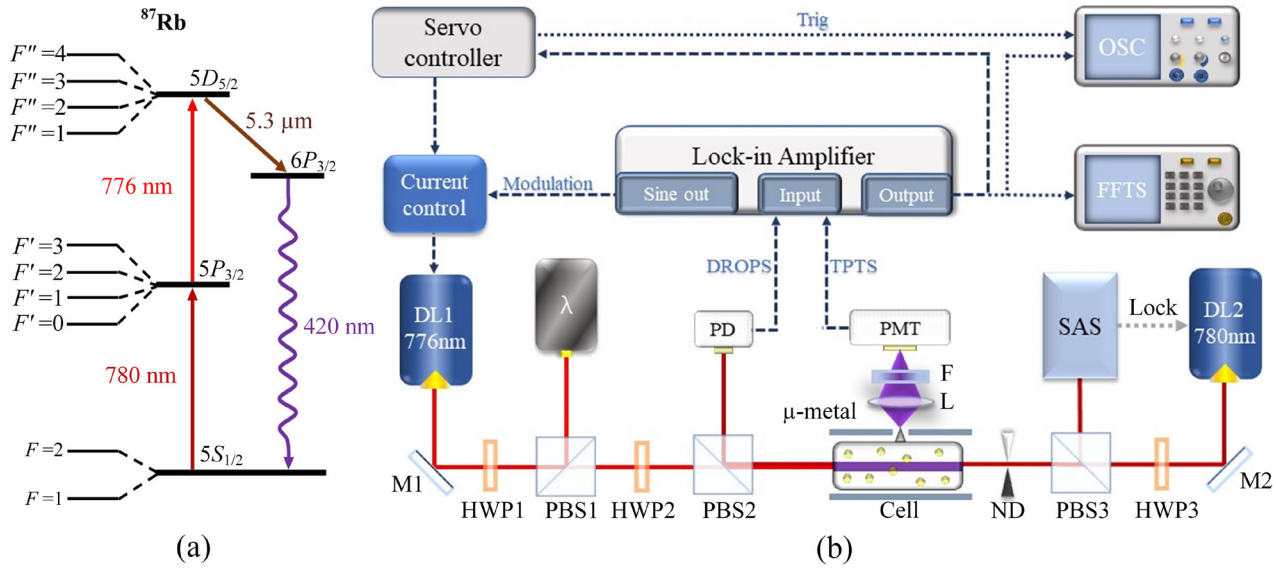

Figure 1. (a) The related energy levels of ^{87}Rb atoms; (b) the schematic of the experiment setup. DL: diode laser, M: mirror, HWP: half-wave plate, QWP: quarter-wave plate, PBS: polarization beam splitter, PD: photodiode, PMT: photomultiplier tube, OSC: oscilloscope, ND: neutral density plate, L: lens, F: 420 nm filter, SAS: saturated absorption spectroscopy, λ: wavelength meter, FFTS: fast Fourier transform spectrum.

cube (CR314-01, Hamamatsu). A 420 nm filter is installed in front of the photomultiplier cube to avoid the stray light entering the photomultiplier cube.

The laser frequency scanning range is about 200 MHz, which covers the $5P \rightarrow 5D$ fine transition. The discriminator voltage, or error signal, is obtained by a lock-in amplifier (SR830, Stanford Research Systems) with the modulation frequency of 50.1 kHz. In the process of obtaining the error signal, the time constant of lock-in amplifier is set as 100 μs and the low pass filter slope is 18 dB. Once the error signal is obtained, it is sent to the controller of the 776 nm laser to achieve the feedback. The current controller is used as an actuator to correct the laser frequency. In this process, the adjusting of the proportion-integration-differential controller of the servo system will result in a better suppress effect of the frequency noise, which is necessary for an optimized frequency stability. Meanwhile, we export error signals to FFTS analyzer to evaluate the stabilization effect. The analysis of the fast Fourier transform of error signal is carried out with the resolution bandwidth of 20 Hz and average count of 10 times.

3. Experimental results and discussion

Once the probe laser is locked on $5S_{1/2}(F = 2) \rightarrow 5P_{3/2}(F' = 3)$ transition while the coupling laser scans around the $5P_{3/2}(F' = 3) \rightarrow 5D_{5/2}$ transition, the original DROPS and TPTS are detected by photodiode and PMT simultaneously. We obtain two spectra with high SNR by controlling the power relationship between 780 nm laser and 776 nm laser [31], which is shown in figures 2(a) and (b). The $5P_{3/2}(F' = 3) \rightarrow 5D_{5/2}(F'' = 1)$ transition, which do not exist in DROPS mechanism for the selection rule, is clearly identified in figure 2(b) and the inset of figure 2(d). This means that TPTS has more frequency references than DROPS around the $5P_{3/2} \rightarrow 5D_{5/2}$ transition. The full width at half maximum of TPTS is 9.26 MHz, which is obviously smaller than 11.86 MHz of DROPS. The discrimination curves of the two methods are also shown in figures 2(c) and (d).

The frequency stabilization capacities of the two methods are characterized by the real-time monitoring of the error signal of the 776 nm laser, which is shown in figure 3. The fluctuation of the error signal represents the residual frequency fluctuation. A slow scan of the 776 nm laser around the $5P_{3/2}(F' = 3) \rightarrow 5D_{5/2}(F'' = 1, 2, 3$ and $4)$ transitions allows a deduced frequency-to-voltage conversion coefficient used for the servo loop. We record the error signal by scanning the laser frequency to obtain a relationship between the error signal voltage and the linewidth of the atomic hyperfine transition, which can be seen in the scanning period of figure 3. The linewidth is obtained from the known interval between two hyperfine transitions. The free running period shows a frequency fluctuation of about 5 MHz with a measurement time of 500 s. After the electrical feedback is applied to the current controller, the frequency of 776 nm laser is stabilized. According to the recording of the voltage fluctuation of the residual error signal, the frequency fluctuation is derived by the relationship of $\delta f/\Delta f = \delta V/V$, where δf and δV are the frequency fluctuation and voltage fluctuation after locking, respectively; and Δf and V are the linewidth and corresponding voltage amplitude of the scanning period, respectively. The residual frequency fluctuation stabilized by DROPS is $\pm$0.4 MHz in 7000 s and in the case of TPTS it is $\pm$0.2 MHz. Although taking a beat with another stable laser is the standard way to evaluate the absolute frequency stability of a locked laser. Under the current condition of only one frequency standard system, the self-comparison by residual error signal is a universal method [15, 32]. It is credible, to some extent, that the self-comparison can estimate the frequency stability of the locked laser.

The stability of frequency locking is assessed by the Allan deviation analysis of the error signal, which is shown in

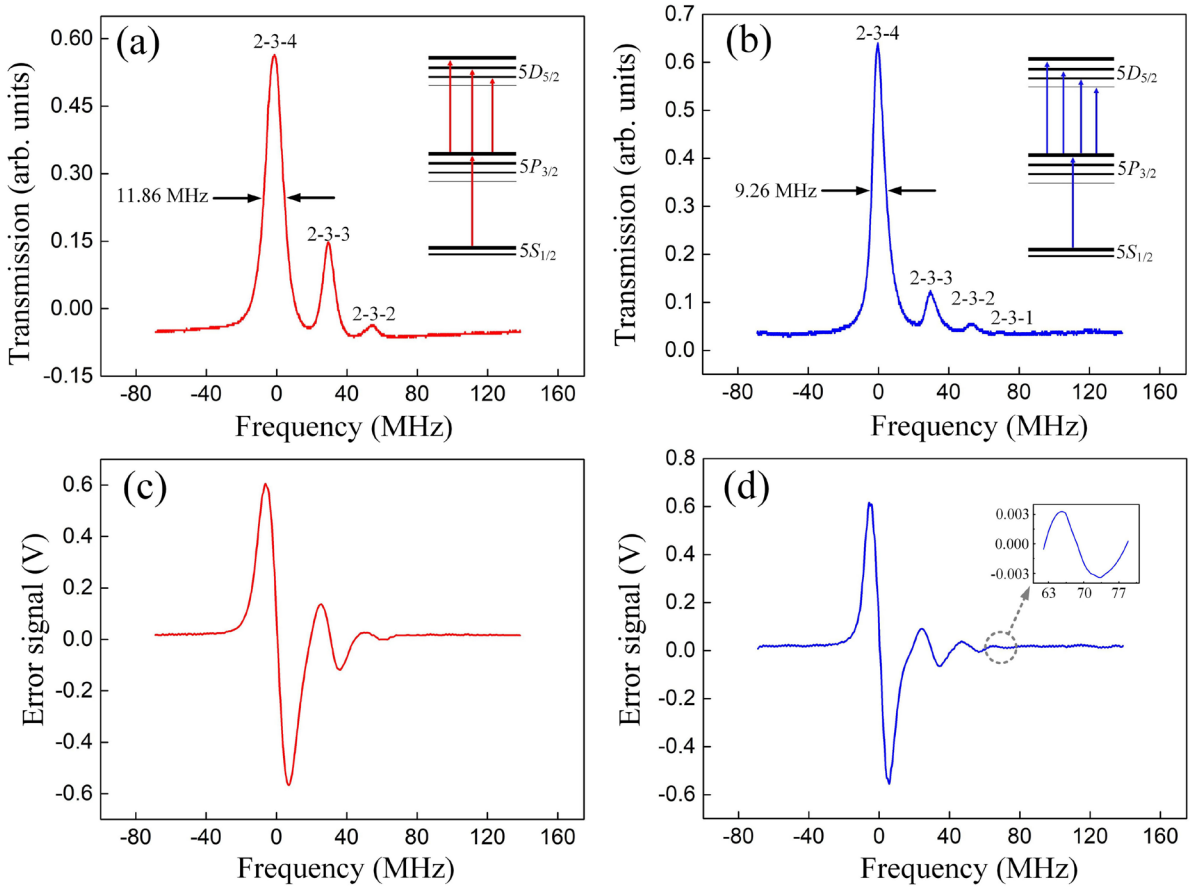

Figure 2. (a) DROPS of $5S_{1/2}(F = 2) \rightarrow 5P_{3/2}(F' = 3) \rightarrow 5D_{5/2}(F'' = 2, 3 \text{ and } 4)$ transition of ^{87}Rb, (b) TPTS of $5S_{1/2}(F = 2) \rightarrow 5P_{3/2}(F' = 3) \rightarrow 5D_{5/2}$ $(F'' = 1, 2, 3 \text{ and } 4)$ transition of ^{87}Rb, (c) discrimination curve of DROPS, (d) discrimination curve of TPTS.

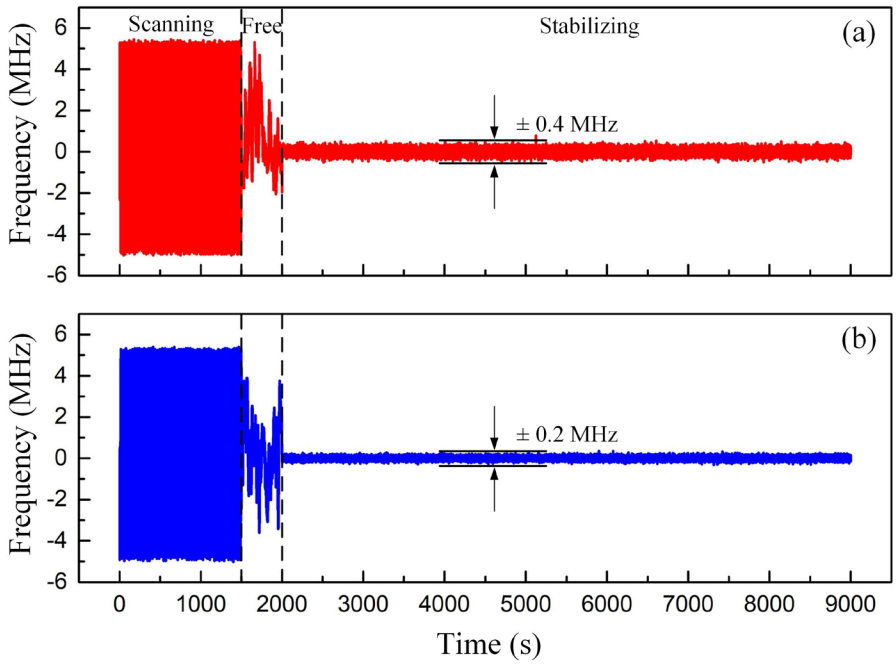

Figure 3. The monitored frequency versus time when the laser is scanning, free running and stabilizing by DROPS (a) and TPTS (b) on the ^{87}Rb $5S_{1/2}(F = 2) \rightarrow 5P_{3/2}(F' = 3) \rightarrow 5D_{5/2}(F'' = 4)$ transition.

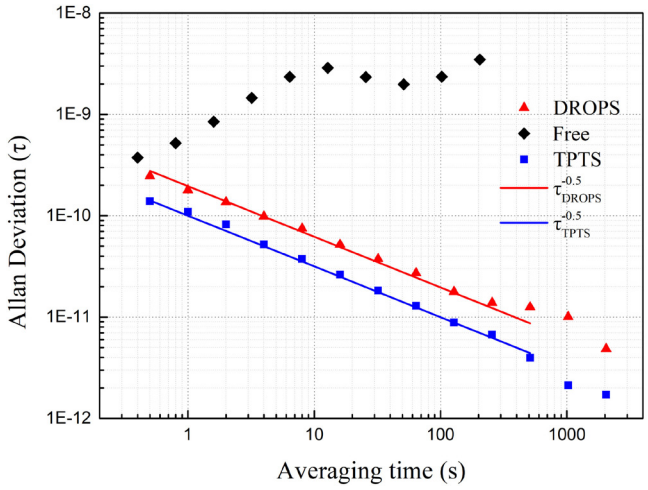

Figure 4. Allan deviation analysis of the residual frequency fluctuations of the stabilized 776 nm laser. The dots are the calculated Allan deviations as a function of the averaging time. The solid lines are the slopes, which enable noise-type identification.

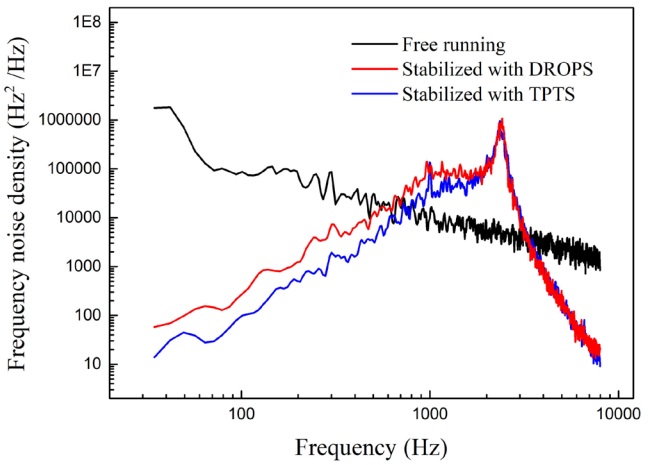

Figure 5. Frequency noise density obtained by fast Fourier transform analysis of the error signals when the 776 nm laser is in the free running period (black curve), stabilized by DROPS (red curve) and TPTS (blue curve), respectively.

figure 4. The Allan deviations exhibit different trends depending on the selected range of averaging times. For the first stage of τ between 0–204 s, the Allan deviation decreases with $1/\tau^{0.5}$, which is typically a white-type frequency noise [33]. The Allan deviation of the DROPS method reaches a floor of 4.86×10^{-12} at an averaging time of 2048 s. However, the Allan deviation of TPTS continuously decreases and finally reaches the floor of 1.71×10^{-12} at an averaging time of 2048 s, which indicates the TPTS has a better locking effect.

Also, the ability of the servo electronics to track frequency fluctuations and keep the laser locked to the resonance is estimated by the analysis of the fast Fourier transform of the error signal, which is shown in figure 5. The FFTS of the two methods are calibrated while fully considering the experimental parameters. The results reveal the residual frequency noise densities of different frequencies with different values. It can clearly be seen that the noise amplitudes of the locking cases are much lower than the free running case at low frequencies (below about 1000 Hz). This phenomenon reflects that the servo feedback controller effectively suppresses additional noise [34]. There is also a drop in the high-frequency part above 3.5 kHz, but that is the result of another reason. Compared to the free running FFTS measured with additional cavity, the high SNR of the error signal must be taken into account when using the lock-in amplifier to obtain the FFTS. So the appropriate lock-in amplifier parameters limit the bandwidths of the error signals and result in a lower frequency noise density than free running. The frequency noise density of both methods of locking cases contain the noise sideband near 2.4 kHz caused by the servo feedback system. This indicates the feedback bandwidth of the system is about 2.4 kHz. We can see that the noise below the noise sideband is significantly suppressed compared to the free running case. If we slightly increase the servo controller gain value, the FFTS fluctuation will increase above the free running noise level. Below this value, the locking of the laser cannot achieve the best result. With the appropriate gain value, the frequency noise densities of the two methods at the near zero point have the minimum value of 10^2 Hz^2/Hz, which represents a good locking effect. Although the frequency noise density analysis is only considered below 8 kHz, this is enough to illustrate the effectiveness of the two locking methods. The low frequency noise is suppressed effectively, especially non-negligible $1/f$ noise and long-term drift caused by temperature and other environmental factors. Obviously, the laser frequency noise of TPTS is suppressed better than DROPS by the servo controller, the narrower full width at half-maximum is the major factor contributes to the better locking effect.

4. Conclusion

In conclusion, we simultaneously obtain the bi-chromatic excitations of the $5D_{5/2}$ level in ^{87}Rb atoms by monitoring the 780 nm probe laser intensity and blue fluorescence emitted from the $6P_{3/2}$ state. DROPS and TPTS are then used to stabilize the 776 nm laser frequency by writing the error signal into the current controller. The resulted residual frequency fluctuation is $\pm$0.4 MHz and $\pm$0.2 MHz in 7000 s, respectively. The locking capacities of the two methods are evaluated by the Allan deviation analysis and fast Fourier transform of error signal, and distinct advantages of TPTS are demonstrated. Narrower full width at half-maximum of TPTS and a higher zero crossing slope by using frequency modulation method lead to a better frequency stabilization. The methods provide the basis for the experimental study of the Rydberg atom and may pave the way for using the frequency standard in optical quantum telecommunication.

Acknowledgments

This work is supported partly by the National Key R&D Program of China under Grant No. 2017YFA0304203; the NSFC under Grants No. 61575116, No. 61875112, No. 61705122, No. 91736209, No. 61728502; the Program for Sanjin

Scholars of Shanxi Province; Applied Basic Research Project of Shanxi Province under Grant No. 201701D221004; Key Research and Development Program of Shanxi Province for International Cooperation under Grant No. 201803D421034 and 1331KSC.

References

[1] Picqué N and Hänsch T W 2019 *Nat. Photon.* **13** 146
[2] Wang X L *et al* 2018 *Phys. Rev. Lett.* **120** 260502
[3] Abbott B P, Jawahar S, Lockerbie N A, Tokmakov K V and LIGO Scientific Collaboration and Virgo Collaboration 2016 *Phys. Rev. Lett.* **116** 061102
[4] Siddons P, Adams C S, Ge C and Hughes I G 2008 *J. Phys. B: At. Mol. Opt. Phys.* **41** 155004
[5] Petelski T, Fattori M, Lamporesi G, Stuhler J and Tino G M 2003 *Eur. Phys. J.* D **22** 279
[6] Wieman C and Hänsch T W 1976 *Phys. Rev. Lett.* **36** 1170
[7] Hall J L, Ma L S, Taubman M, Tiemann B, Hong F L, Pfister O and Ye J 1999 *IEEE Trans. Instrum. Meas.* **48** 583
[8] Young B C, Cruz F C, Itano W M and Bergquist J C 1999 *Phys. Rev. Lett.* **82** 3799
[9] Cundiff S T and Ye J 2003 *Rev. Mod. Phys.* **75** 325
[10] Matei D G *et al* 2017 *Phys. Rev. Lett.* **118** 263202
[11] Su D, Meng T, Ji Z, Yuan J, Zhao Y, Xiao L and Jia S 2014 *Appl. Opt.* **53** 7011
[12] Yuan J, Li Y, Li S, Li C, Wang L, Xiao L and Jia S 2017 *Laser Phys. Lett.* **14** 125206
[13] Yuan J, Wu C, Wang L, Chen G and Jia S 2019 *Opt. Lett.* **44** 4123
[14] Affolderbach C and Mileti G 2005 *Rev. Sci. Instrum.* **76** 073108
[15] Zhang S, Zhang X, Cui J, Jiang Z, Shang H, Zhu C, Chang P, Zhang L, Tu J and Chen J 2017 *Rev. Sci. Instrum.* **88** 103106
[16] Shang H, Zhang X, Zhang S, Pan D, Chen H and Chen J 2017 *Opt. Express* **25** 30459
[17] Martin K W, Phelps G, Lemke N D, Bigelow M S, Stuhl B, Wojcik M, Holt M, Coddington I, Bishop M W and Burke J H 2018 *Phys. Rev. Appl.* **9** 014019
[18] Kalatskiy A Y, Afanasiev A E, Melentiev P N and Balykin V I 2017 *Laser Phys.* **27** 055703
[19] Wang S, Yuan J, Wang L, Xiao L and Jia S 2018 *J. Phys. Soc. Japan* **87** 084301
[20] Yuan J, Wu C, Li Y, Wang L, Zhang Y, Xiao L and Jia S 2019 *Opt. Express* **27** 92
[21] Offer R F, Stulga D, Riis E, Franke-Arnold S and Arnold A S 2018 *Commun. Phys.* **1** 84
[22] Chanelière T, Matsukevich D N, Jenkins S D, Kennedy T A B, Chapman M S and Kuzmich A 2006 *Phys. Rev. Lett.* **96** 093604
[23] Xue Y, Hao L, Jiao Y, Han X, Bai S, Zhao J and Raithel G 2019 *Phys. Rev.* A **99** 053426
[24] Bao S, Zhang H, Zhou J, Zhang L, Zhao J, Xiao L and Jia S 2017 *Laser Phys.* **27** 015701
[25] Hang C, Li W and Huang G 2019 *Phy. Rev.* A **100** 043807
[26] Moon H S, Lee L, Kim K and Kim J B 2004 *Appl. Phys. Lett.* **85** 3965
[27] Moon H S, Lee L, Kim K and Kim J B 2004 *Appl. Phys. Lett.* **84** 3001
[28] Akulshin A M, Hall B V, Ivannikov V, Orel A A and Sidorov A I 2011 *J. Phys. B: At. Mol. Opt. Phys.* **44** 215401
[29] Terra O and Hussein H 2016 *Appl. Phys.* B **122** 27
[30] Heavens O S 1961 *J. Opt. Soc. Am.* **51** 1058
[31] Li Y, Li S, Yuan J, Wang L, Xiao L and Jia S 2018 *Chin. Phys. Lett.* **35** 093201
[32] Nicholson T L *et al* 2015 *Nat. Commun.* **6** 6896
[33] Dinesan H, Fasci E, Castrillo A and Gianfrani L 2014 *Opt. Lett.* **39** 2198
[34] Dumont P, Camargo F, Danet J M, Holleville D and Guerandel S 2014 *J. Lightwave Technol.* **32** 3817